J Polym Res (2013) 20:326
DOI 10.1007/s10965-013-0326-y

ORIGINAL PAPER

Piezoresistive response of carbon nanotubes-polyamides composites processed by extrusion

L. Arboleda · A. Ares · M. J. Abad · A. Ferreira · P. Costa · S. Lanceros-Mendez

Received: 6 September 2013 / Accepted: 14 November 2013 / Published online: 30 November 2013

Abstract The piezoresistive response of carbon nanotube (CNT)-polyamide composites processed by extrusion has been investigated as a function of CNT amount, polyamide 66 (PA66) / polyamide 6 (PA6) ratio, within the matrix and the masterbatch used to incorporate the CNT into the composite (PA66 masterbatch or PA6 masterbatch). The dispersion level of CNT in PA66/PA6 matrix was evaluated and related with the thermal, electrical and electromechanical properties. It is concluded that the inclusion of the CNT in the PA6 masterbatch helps to improve dispersion leading to larger values of the electrical conductivity in the composites prepared with larger PA66 content. On the other hand, the Gauge Factor (GF), which provides the sensitivity of a piezoresistive sensor, is larger for composites prepared from the PA66 masterbatch. The increase of PA66 content improving also the electromechanical response and GF reaches values up to 6. This fact demonstrates the suitability of the materials for sensor applications produced in an up-scaled production way.

Keywords Piezoresistive · Gauge factor · Carbon nanotubes composites · Polyamides

Introduction

Most polymers are known for their excellent insulating properties. Nevertheless increasing number of applications demand from these materials dissipative or conductive characteristics. In this way, intrinsic conductive polymers and conductive composites based on conductive fillers such as carbon nanotubes (CNTs) and polymer matrices have been developed as functional components in the manufacture of sensors, microelectrodes, electromagnetic shielding, electroconductive rubbers and electrostatically paintable materials, among others [1].

Enhanced conductivity in polymers can be thus achieved either using inherently conductive polymers or adding electrical conductive fillers to the polymer matrix. Polyaniline, polypyrrole or polythiophene are, among others, inherently conductive polymers due to their conjugated π-electron system [2]. With these materials, transparent electrical conductive polymer films have been achieved, which are widely used, for example, in organic solar cells [3]. The main drawbacks of these materials are their high prices, the difficulties in melt compounding due to nonmeltability combined with thermal degradation, and their poor long-term stability.

In a second approach, electrical conductive fillers are incorporated in the polymer matrix. Above certain filler content, the electrical percolation threshold is achieved at which the conductive filler particles form electrical pathways through the polymer matrix. As conductive fillers, metal powders and carbon based additives are quite commonly used in industry [4].

Within this family, carbon nanotubes (CNTs) are known to produce composites with superior electrical and mechanical properties when compared to other carbon allotropes such as carbon black (CB) or carbon nanofibers (CNF) [5]. Strong increases in electrical conductivity and mechanical properties can be obtained in polymer nanocomposites with CNT concentrations below 5 wt.% [6–8].

Electrical, thermal and mechanical properties of the composites are affected both by the characteristics of the CNT and also by the processing technique used to prepare the polymer

L. Arboleda · A. Ares · M. J. Abad (✉)
Grupo de Polímeros, University of A Coruña, CIT- Campus de Esteiro, 15403 Ferrol, Spain
e-mail: mjabad@udc.es

A. Ferreira · P. Costa · S. Lanceros-Mendez
Center/Department of Physics, University of Minho, Campus de Gualtar, 4710-057 Braga, Portugal

composite [9]. Effective use of the full potential of nanotubes to enhance the electrical conductivity of polymer composites depends primarily on the ability to disperse the nanotubes in the polymer matrix. Due to intermolecular van der Waals interactions and entanglement between the nanotubes, destruction of primary agglomerates is not easily obtained [10].

Several methods have been used to solve this problem and, for example, in situ-polymerization is a method to generate composites with well-dispersed nanotubes [11, 12].

However, this and similar approaches are not industrial-scale technically feasible solutions. Instead, if the composites are prepared using the melt mixing method, the results obtained can be easily scale up to an industrial level. In that case, the number and size of primary agglomerates can be minimized by appropriate application of shear during melt mixing [13–15]. Thus, it has been proven for many systems such as polycarbonate (PC) filled with multiwalled carbon nanotubes (MWCNT) that the processing by extrusion or injection moulding [16, 17], as well as the post mixing processing (e.g., sample manufacture) [18, 19] strongly influences the final properties of the composite, since the processing parameters influence the characteristics of the CNT network.

Usually, low electrical resistivity values of the composite are related to a more perfect conductive filler network formation related to an appropriate dispersion of CNTs or CNT clusters into the polymer matrix. A complete characterization of this network is quite difficult. Large aggregates resulting from non-dispersed primary agglomerates formed during inappropriate mixing can be observed by optical light microscopy (LM) [20] or scanning electron microscopy (SEM) [21]. Nevertheless, to properly examine CNT dispersion at the submicron scale and polymer-CNT interface, transmission electron microscopy (TEM) is commonly necessary, despite the drawbacks of not allowing a complete visualization of the complex three-dimensional structure of the individual nanotubes or their aggregates [10] by showing just a quite small section of the composite.

In recent years, CNT/polymer composites are gaining attention for smart materials applications [22–24] and in particular for the development for piezoresistive sensors for structural health monitoring systems [22, 23, 25], among others [26]. Several matrix such as thermoplastic poly(vinylidene fluoride) [27] and polymethylmethacrylate (PMMA) [24], thermoplastic elastomers such as silicone rubber or tri-block copolymer styrene-butadiene-styrene (SBS) [26, 28] and epoxy resins [21], composites with CNT or carbon nanofibers have been prepared using laboratory methods and piezoresistive properties have been obtained that indicate the suitability of the materials for strain and pressure sensor applications. The gauge factor of these composite samples strongly depend of matrix, carbon nanofiller type and content [23, 26] reaching values up to 1.4 to 15.3 [1] for thermoplastics, 0.6 to 2.2 for epoxy resins [29] and 1 to 6 for some elastomers [1].

Polyamides (PA) are semi-crystalline polymers particularly interesting as composite matrices due to their versatility and ease of processing [30]. Polyamides are tough and have excellent sliding and wear characteristics. Properties vary from the hard and tough PA 66 to the soft and flexible PA 12. Depending on the type, polyamides absorb different amounts of moisture, which also affect the mechanical characteristics and electrical response [31, 32].

The influence of MWCNT addition in PA6 or PA66 properties has been addressed. One part of these studies has been focused on relationships among the processing parameters used to prepare the nanocomposites (rotation speed, time and mixing temperature) and electrical properties and crystallization behaviour of the polymer composites [30] in order to obtain lowest electrical volume resistivity. A high mixing temperature, a low rotation speed, and a high mixing time were found to be the best conditions. Moreover, MWCNTs can modify the crystallization temperature of the polyamide matrix and, consequently, its crystalline degree [33, 34]. The effect of different reactive couplings or modifiers on electrical, rheological and morphological behavior of polyamide/CNT composites has been also reported [35, 36].

Despite the wide bibliography with respect of carbon nanotubes-polyamides composites both in PA66 and PA6, the study of blends with different ratios of these polyamides and different CNT content has been scarcely explored, despite the potential advantages in tailoring materials properties for specific applications taken into account the different materials characteristics.

Further, for upscaling processes and industrial applications it is important where and how the nanofiller is incorporated [35]. In the case of a polymer blend the fillers can be incorporated in either of the constituent masterbatches.

Therefore, this work reports on the dispersion level, thermal behaviour, electrical conductivity and electromechanical performance of polyamides/multi-wall carbon nanotubes (PA66/PA6/MWCNT) composites processed by extrusion. Different PA66/PA6 ratios are investigated as well as different CNT contents incorporated from PA66 or PA6 masterbatches, respectively.

This work is relevant as it demonstrates the feasibility of the polymer composites for the development of piezoresistive sensors that can be processed with standard up-scalable polymer processing techniques.

Experimental

Materials

The polymers used in this work were polyamide PA66 (PA66 Dinalon of Repol) and PA6 (Zytel of DuPont) with a density

of 1.13 g/cm^3 and 1.14 g/cm^3 and a melt flow rate of 68 and 95 g/10 min (290 °C, 2.16 kg), respectively. A masterbatch of 15 wt.% MWCNT dispersed in PA66 and another one of 15 wt.% MWCNT dispersed in PA6 were supplied by Nanocyl, Sambrevile, Belgium, in pellets form. The polyamides used in masterbatchs are similar to the polyamides added in the extruder blends. The CNTs are characterized according to the supplier by an average diameter of 9.5 nm, an average length of 1.5 μm, a carbon purity of 90 % and a surface area of 250–300 m^2/g.

Preparation of composites

Previous to the blending, the masterbatches and the two polyamides were dried in an oven at 110 °C for 6 h. To prepare the different formulations, the corresponding masterbatch was diluted with different contents of PA66 and PA6 to reach the desired ratio between the polyamides and the different MWCNT contents. Then, composites with different contents of MWCNTs and different ratios of polyamides were prepared using a co-rotating twin-screw extruder (Brabender DSE 20) operating at 20 rpm, with a barrel temperature of 255–270 °C and a die temperature of 260 °C. All the components (virgin polyamides and masterbatch) were premixed by tumbling and fed simultaneously into the extruder. The obtained pellets were compression moulded into 2 mm plaques at 285 °C applying a pressure of 40 bar for 10 min. Finally, the plaques were cooled down by circulating water within the press plates under a pressure of 25 bar for 5 min.

Table 1 shows the composite formulations and the MWCNT content with respect to the overall polyamide content.

Morphological analysis by scanning electron microscopy

The composite morphology was analysed by scanning electron microscopy (SEM). For SEM analysis, some specimens were cryo-fractured in liquid nitrogen and the fracture surfaces examined using a JEOL JSM-6400 scanning electron microscope (SEM) at an accelerating voltage of 20 kV. The samples were previously sputter-coated with a thin layer of gold.

Table 1 Prepared composites of PA66/PA6 with different contents of CNT, in weight. MB indicates the matrix from which the nanotubes were dispersed in each sample

PA66/PA6/CNT	PA66 (wt.%)	PA6 (wt.%)	CNT (wt.%)
50/50 (MB)/1	49.50	49.50	1
50/50 (MB)/3	48.50	48.50	3
50/50 (MB)/5	47.50	47.50	5
50/50 (MB)/7.5	46.25	46.25	7.5
75 (MB)/25/3	72.75	24.25	3
25 (MB)/75/3	24.25	72.75	3
75/25 (MB)/3	72.75	24.25	3
25/75 (MB)/3	24.25	72.75	3

Thermal analysis

Thermal measurements were carried out with a differential scanning calorimeter (DSC-7, Perkin-Elmer) under nitrogen atmosphere. The samples (6–10 mg) were heated from 10 °C to 280 °C at a heating rate of 10 °C.min^{-1}.

Heating-cooling-heating cycles were performed for the different samples. The first heating scan was used to determine the melting temperature (T_m) and the heat of melting (ΔH_m). To allow comparison between samples with different MWCNT contents, the melting enthalpies (ΔH_m) were normalized to the polyamide fraction, further, a deconvolution procedure was applied to the melting thermograms to better understand the effects of nanotubes on the crystalline phase of each polyamide type. The degree of crystallinity (X_c) was calculated with Eq. 1:

$$X_c = \Delta H_m * 100 / \Delta H_0 * \omega_p \quad (1)$$

where ΔH_m is the melting enthalpy of sample, ω_p, weigh fraction of the corresponding polyamide, assuming $\Delta H_0 =$ 230 J/g for 100 % crystalline PA6 [37] and $\Delta H_0 =$ 190 J/g for 100 % crystalline PA66 [38].

Electrical conductivity measurement

Direct current (DC) electrical surface resistance measurements at room temperature were performed in rectangular samples with the dimensions 70×10×2 mm with a 4 prove method with a Keithley 487 picoammeter/voltage source. Previously, two parallel rectangular gold electrodes of 6×1 mm were deposited by magnetron sputtering. Copper wires were attached to the electrodes with silver paste to ensure good electrical contact. The surface resistivity ρ_s (Ω/sq) was calculated from:

$$\rho_S = \frac{R l_e}{d_e} \quad (2)$$

where R is the surface resistance in Ω, l_e is the electrode length and d_e is the distance between electrodes.

Electro-mechanical characterization

The sensitivity of a piezoresistive sensor can be quantified through the gauge factor (GF), which is defined as the relative

change in electrical resistance due to an applied mechanical deformation:

$$GF = \frac{dR/R}{dl/l} \tag{3}$$

where R is the electrical resistance of the material without deformation and dR is the resistance change caused by the change dl in length (l) [39]. In the surface sensing mode, the GF can be written as:

$$GF = \frac{dR/R}{\varepsilon_l} = \frac{d\rho/\rho}{\varepsilon_l} + 1 + \nu \tag{4}$$

where $dl/l = \varepsilon_l$ and ν is the Poisson modulus of the material. Equation (3) shows that two effects contribute to the gauge factor: an intrinsic piezoresistive effect $((d\rho/\rho)/\varepsilon_l)$ and a geometric effect $(1+\nu)$ [39].

Electro-mechanical experiments were performed under 4-point-bending mechanical solicitation (Fig. 1) using a universal mechanical tests Shimadzu-AG-IS while simultaneously recording the electrical resistance variation of the samples with a Agilent 34401A multimeter. The electromechanical measures of samples were calculated using Eq. (2).

The strain, calculated from the theory of pure bending of a plate to a cylindrical surface, valid between the inner loading points (Fig. 1), is given by [40]:

$$\varepsilon = \frac{3dz}{5a^2} \tag{5}$$

Four loading and unloading cycles were performed for each sample at different z-displacements between 0.3 and 1 mm, deformation speeds between 1 and 50 mm/min and temperatures from 25 to 100 °C. The GF value was calculated for each cycle, from the z-displacement and the electrical resistance curves, by linear regression. Finally, the average value of the GF was calculated for each sample. The calculated value of the GF for the up or down mechanical cycles was the same, unless specifically specified.

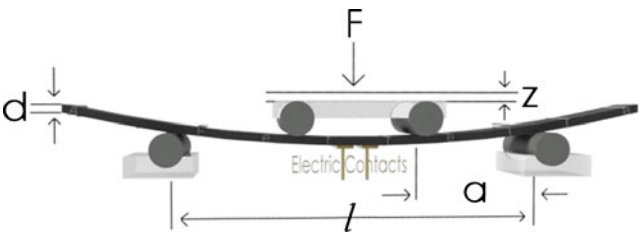

Fig. 1 Schematic representation of the 4-point bending tests: z is the vertical displacement of the piston, d is the thickness of the sample, a is the distance between the first and the second bending points (15 mm) and l the distance between the lower supports (45 mm)

Results and discussion

In the following, the main results are presented and discussed in terms of the influence of masterbatch type, filler content and polyamide ratio on the microscopic characteristics, thermal behavior and electrical and electromechanical response of the samples.

Morphological characteristics

Figure 2 shows the SEM images of composites with two different masterbatches (PA6 and PA66), different polyamide ratio but with the same concentration of filler (3 wt.% CNT). A similar dispersion level of carbon nanotubes is obtained for all composite samples. In this way, for 50/50 (MB) and different filler contents (1 % to 7.5 %), Fig. 1a, b and c show that the carbon nanotubes are disperse homogeneously. In a similar way, for PA66 masterbatch and different PA66/PA6 ratios and 3 % filler content, Fig. 1e and f do not show agglomerates and the nanotubes are well distributed in the composite samples.

Differences are nevertheless obtained when comparing composites with different PA66/PA6 ratios with 3 wt.% CNT, a better dispersion of fillers being reached with higher content of PA66 and using PA6 masterbatch (75/25(MB)/3) (Fig. 1d). This fact is attributed to the higher melting viscosity of PA66 when compared to PA6, as it has been proven that the most effective dispersion and distribution of primary MWCNT agglomerates was obtained when using high viscosity matrices albeit this could also result in increased nanotube shortening as compared to the use of lower viscosity matrices [10]. In the present case, the pre-dispersion of MWCNT in a low viscosity matrix as PA6, avoids this drawback, as the applied shear strength is reduced during the melt mixing.

The opposite behaviour is observed in the 25(MB)/75/3 composite (Fig. 1e). In this case, the nanotubes mixed from a PA66 masterbatch during extrusion are more difficultly dispersed in the polymer matrix. The higher content of PA6, with a lower melt viscosity, is not able to generate shear enough to disperse uniformly the nanotubes during the extrusion.

Comparing 1b and 1d SEM images the only and exclusively influence of PA66 content could be analysed since the masterbatch type and CNT amount is the same in the two composites. In this case, a better dispersion in the sample with a higher content of PA66 was obtained. On the other hand, if composites with the same ratio of polyamides (75/25) and the same CNT amount, such as 1d and 1f images, are compared, the influence of masterbatch could be analysed and the better dispersion has been got when MWCNT are initially predispersed in the low viscosity matrix.

The micrographs 1b and 1f show an intermediate behaviour. It is thus concluded that a higher content of PA66 improves the CNT dispersion, but if nanotubes are pre

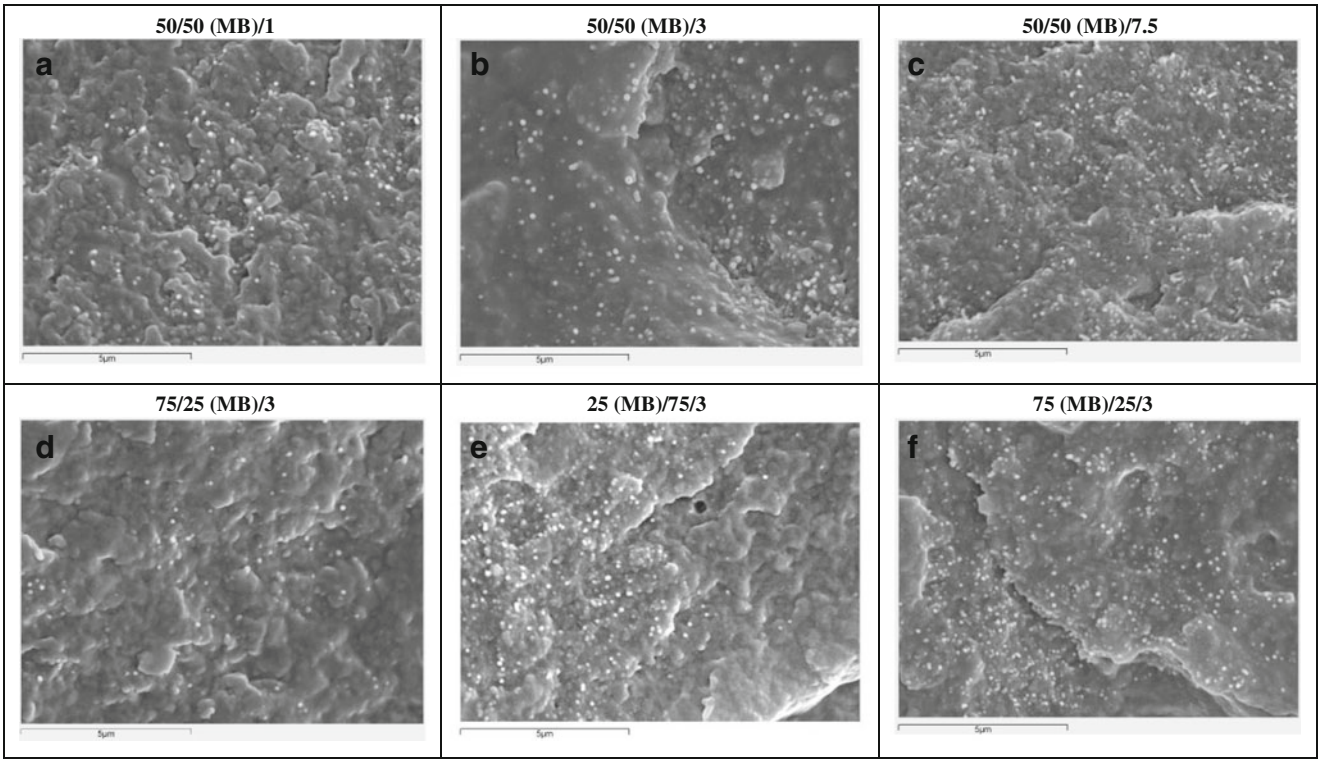

Fig. 2 SEM images for several PA66/PA6 (25/75, 50/50 and 75/25) blends and CNT content (1, 3 and 7.5 %)

dispersed in a masterbatch of low viscosity, the effect can be further improved.

In conclusion, two important factors with a clear influence on observed CNT dispersion and distribution have appeared: on one side the content of PA66, the matrix with higher viscosity in the composites and on the other hand the nanotubes must be included originally in a lower viscosity matrix. Keeping in mind the obtained electrical results detailed in section 3.3, we could suspect which one between these two aspects is more important for achieve the best conductivity values.

Thermal properties

Both polyamides are miscible in the amorphous state within the range of processing temperatures [41]. However, during cooling, polyamides are able to form different crystalline structures, which could be modified by the presence of CNT [33]. In order to evaluate these aspects and their influence in the electrical and electromechanical behavior of the composites, the DSC analysis was limited to the first heating scan on samples processed in similar conditions as the ones to be used for the different characterization tests and thus with the same thermal history.

As observed in the DSC thermograms (Fig. 3) and the corresponding data of Table 2 the crystallization of both polyamides depends on their ratio in the composite. Whereas for 50/50 and 25/75 ratios both polyamides form two separated melting peaks during sample cooling, for the 75/25 ratio the PA6 crystallization is inhibited by the larger proportion of PA66. A single melting peak, corresponding to the PA66 melt is shown in this sample. On the other hand, the degree of crystallization of both polyamides decreases when they are blended, the drop being more important in PA6. This fact can be attributed to the low viscosity of this polyamide, together with the miscibility with PA66 that, for certain relative concentrations of the polymers, encourages the diffusion of PA6 molecules within the PA66 matrix in the amorphous state, inhibiting the crystal formation [42].

For composites with equal quantity of the two polymers, the melting temperatures of both polyamides and the degree of crystallinity, Xc, of PA66 decreases as a function of CNT content. The drop is more significant at low loadings. Although, it has been reported the nucleating effect of CNTs in polyamide matrices which can lead to an increase of the degree of crystallinity, in the present case this does not happen. With the combination of two polyamides with CNTs, the polymers are less able to diffuse in order to form crystalline structures. The decrease in the melting temperatures and crystalline degree with filler addition suggests that the crystallization of both polyamides is heterogeneous and the crystals formed are thinner [43].

For composites with 75/25 and 25/75 ratios, the crystallization of the polyamide in lower proportion is inhibited by the

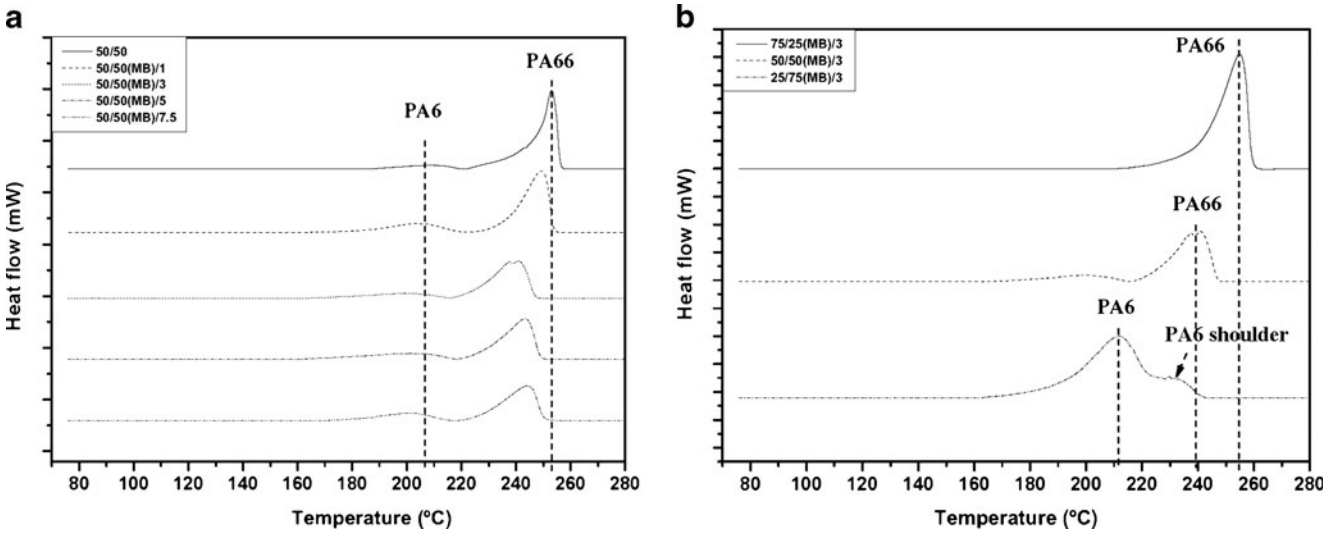

Fig. 3 DSC scans of composites samples for **a** PA66/PA6 (50/50) for CNT content up to 7.5 %, and **b** PA66/6 for 25/75, 50/50 and 75/25 ratios with 3 % CNT

presence of the fillers. The melting thermograms show thus a single peak corresponding to the polyamide in the larger quantity (Fig. 3). This behaviour seems to be related to the crystallization kinetic [43]. The low nanotube content (3 wt.%) encourages the crystals growth in the dominant polyamide. On the other hand, the crystallization of the other polyamide would be more difficult since it is diluted on the whole material as a secondary phase.

When the polyamide ratio is 50/50, the growth of crystals of both polyamides is affected by the presence of crystals of the other one. The growth of one limiting the growth of the other one. Because of this, the degree of crystallinity and the melting temperatures are lower than when one or the other polyamide is dominant in the composite. This effect is more important for PA6 as it crystallizes at lower temperatures, when PA66 is already crystallized.

Finally, the observed behaviour appears to be independent of the masterbatch used to disperse the nanotubes. The only difference was observed in the 25/75(MB)/3 sample, which displays a double peak when the CNTs are mixed from a PA6 masterbatch with respect to its twin sample (25(MB)/75/3), using a PA66 masterbatch. Again, differences in viscosity of the matrices and sample morphology (as discussed earlier) are at the origin of the different species of crystals formed in this sample.

For pure polyamides and all composites, the melting properties are summarized in Table 2.

Electrical properties

The composites with masterbatch PA6 with different PA66/PA6 ratios and CNT contents are shown in Fig. 4a. The

Table 2 Melting properties of PA6 and Pa66 for the different composites samples. R^2 is the regression coefficient obtained for the fitting

PA66/PA6/CNT	Tm $_{PA6}$ (°C)	$\Delta H_{m\ PA6}$ (J/g $_{PA6}$)	Xc $_{PA6}$ (%)	Tm $_{PA66}$ (°C)	$\Delta H_{m\ PA66}$ (J/g $_{PA66}$)	Xc $_{PA66}$ (%)	R^2
PA6	217.6	75.9	33.0	–	–	–	–
PA66	–	–	–	258.9	91.5	48.2	–
50/50	206.8	14.6	6.3	252.0	101.2	53.3	0.961
50/50(MB)/1	202.0	25.4	11.0	247.5	87.7	46.2	0.930
50/50(MB)/3	195.3	15.5	6.7	237.9 (240.9)	68.4	36.0	0.932
50/50(MB)/5	196.2	27.4	11.9	240.6	66.3	34.9	0.982
50/50(MB)/7.5	198.5	21.8	9.5	241.9	65.5	34.5	0.931
75/25	207.1	80.8	35.1	253.8	77.2	40.6	0.898
75(MB)/25/3	–	–	–	248.6	82.1	43.2	0.908
75/25(MB)/3	–	–	–	252.7	84.5	44.5	0.912
25/75	218.2	33.5	14.6	247.9	83.2	43.8	0.938
25(MB)/75/3	214.1	75.5	32.8	–	–	–	0.957
25/75(MB)/3	210.5 (229.7)[a]	105.2	45.7	–	–	–	0.983

[a] PA6 shoulder

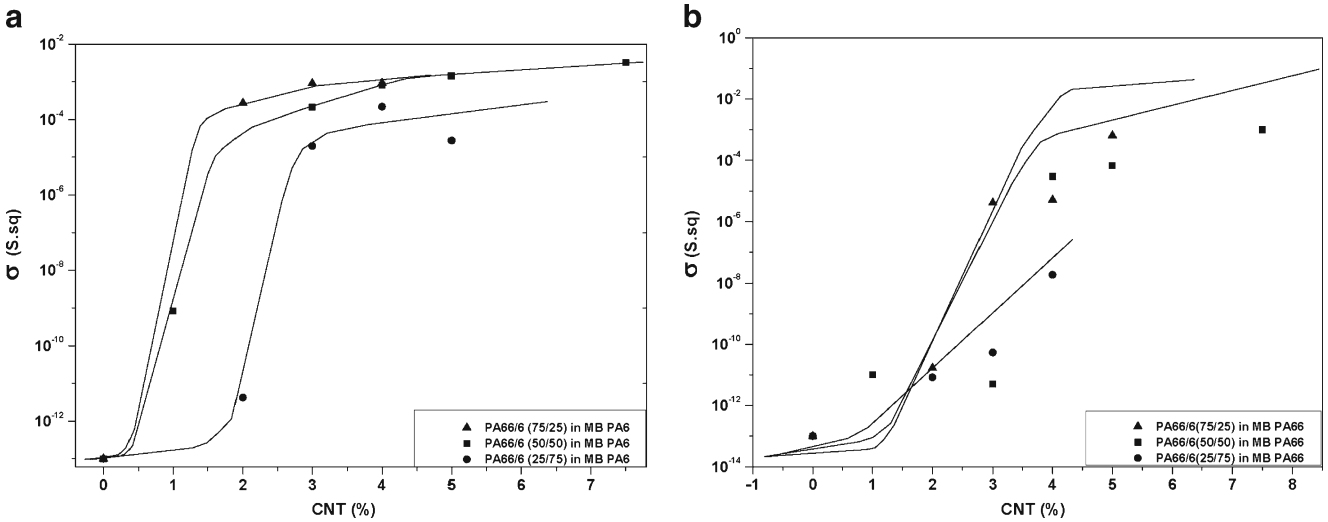

Fig. 4 Electrical conductivity for composite samples with CNT up to 7.5 % and polyamide ratios 75/25, 50/50 and 25/75 in masterbatch PA6 (**a**) and PA66 (**b**). The lines are for guiding the eyes

electrical conductivity increases with CNT content for the three PA ratios, 75/25, 50/50 and 25/75 and the conductivity values also increase with increasing PA66 content in the composites. The presence of PA66 also decreases percolation threshold in the composites samples from 3 wt.% CNT for the 25/75 ratio composites to 2 % CNT in the composites with 75/25 ratio.

Figure 4b shows the electrical behaviour for the CNT composites obtained from PA66 masterbatch. The trend in conductivity with different PA66/PA6 ratios is similar to the one obtained for the PA6 masterbatch, but comparing the same CNT quantities; the values of the electrical conductivity are lower.

The explanation for this behavior is related with the differences in CNT dispersion observed (Fig. 2). As previously stated, the nanocomposite with 75/25 polyamide ratio using PA6 masterbatch, results in the best dispersion of CNT in the polyamide matrix, due to the combination of higher quantity of PA66 (with high melt viscosity) and CNT pre-dispersed in PA6 masterbatch (with lower melt viscosity), and this better dispersion of the CNT improves the electrical conductivity.

As previously mentioned, there are two factors which have a clear influence on nanotube dispersion and distribution: on one side the content of PA66, the matrix with higher viscosity, in the composites and, on the other hand, the fact of the nanotubes are originally included in a lower viscosity matrix. In view of the result obtained, in this case, the fact of MWCNT are predispersed in a matrix with lower viscosity is more decisive for achieve the best conductivity values.

Piezoresistive properties

The piezoresistive properties of the composites are measured in 4-point bending tests, studying the influence of the different masterbatch, polyamide ratio, and filler content.

Typical experiments with 4 loading-unloading mechanical cycles with simultaneous measurements of the electrical resistance variation are shown in Fig. 5a. For each loading and unloading electromechanical tests a linear fit was performed for obtaining the value of the GF, as shown in Fig. 5b. As observed in Fig. 5, proper linearity between mechanical strains and electrical resistance variation is obtained, indicating the suitability of the materials for sensor applications.

The behavior of the GF for the different composites samples is presented in Fig. 6.

For the composites prepared from the PA66 masterbatch the GF is higher for 75(MB)/25 samples, with a maximum value of GF ~ 6, for 3 % and 5 % CNT (Fig. 6a). For equal amounts of polyamides (50/50) (Fig. 6a) the GF is less than 2 for low CNT contents and increase to a maximum of ~3 with higher CNT loading. For the samples prepared from the PA6 masterbatch (Fig. 6b), the GF is in general lower and less dependent both on the relative polyamide and filler contents than in the case of the PA66 masterbatch. It is thus concluded that the preparation of the composites from the PA66 masterbatch and the increase of PA66 content in these samples improves the electromechanical response of the composites. This fact is in contrast to the fact that the best values of the electrical conductivity are obtained for the PA6 masterbatch with large PA66 content. The explanation for this behavior is again related to the differences in CNT dispersion (Fig. 2). Samples prepared from the PA6 masterbatch, show best dispersion of CNT in the polyamide matrix, which lead to better values of the conductivity but less variation of the conductive paths when the material is under mechanical deformation, the latter being at the basis of the electromechanical response and being the reason why the larger GF are typically obtained close to the percolation threshold [20, 27].

In the present case, due to the complex topology of the polymer microstructure, related to the different masterbatches

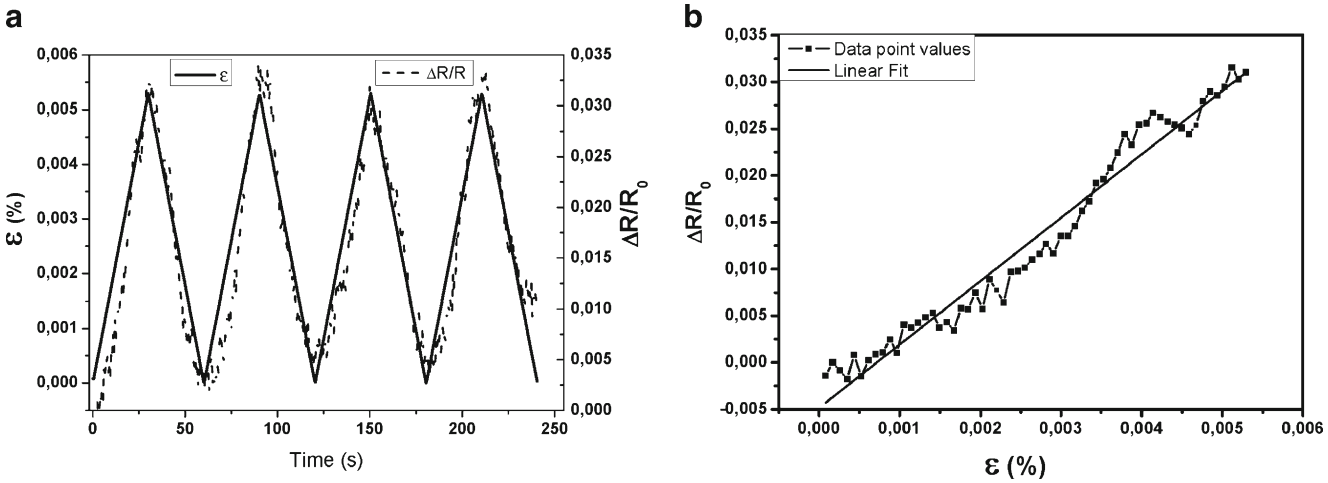

Fig. 5 **a** Variation of relative electrical resistance and mechanical strain over time for 75(MB)/25/3 composites during 4 loading and unloading cycles. **b** Linear fit of relative electrical resistance and strain in the 75(MB)/25/3 composite

and the different polymer characteristics (e.g. mechanical and crystalline characteristics of each phase within the blend), no specific trend is obtained (Fig. 6). In any case, two important conclusions are drawn: first, the presence of PA66 improves the electromechanical response leading to large GF compatible with the upscale production of piezoresistive sensors, as the observed GF are among the largest obtained in the literature for thermoplastic composites due to a larger contribution of intrinsic piezoresistive response [44–47]; second, that the GF is not as strongly dependent on CNT concentration as in similar thermoplastic composites [47] and that the larger values of the GF are not related to the percolation threshold, indicating a complex blend topology and therefore CNT network characteristics.

To assess the application potential of the composites, the 75(MB)/25/3 sample was analyzed by performing electromechanical tests as a function of temperature, from room temperature to 100 °C, for deformation speeds up to until 50 mm/min and different maximum strains.

With respect to the temperature behavior (Fig. 7) the GF strongly decreases from the room temperature value above 5 to ~3.5 at 40 °C remaining this value stable until 100 °C. The large GF values, in the temperature range from room temperature to 100 °C, prove the suitability of the material for applications. The decrease of the GF around 40 °C is not related to any temperature induced transition of the polymer and thus can only be attributed to an annealing effect leading

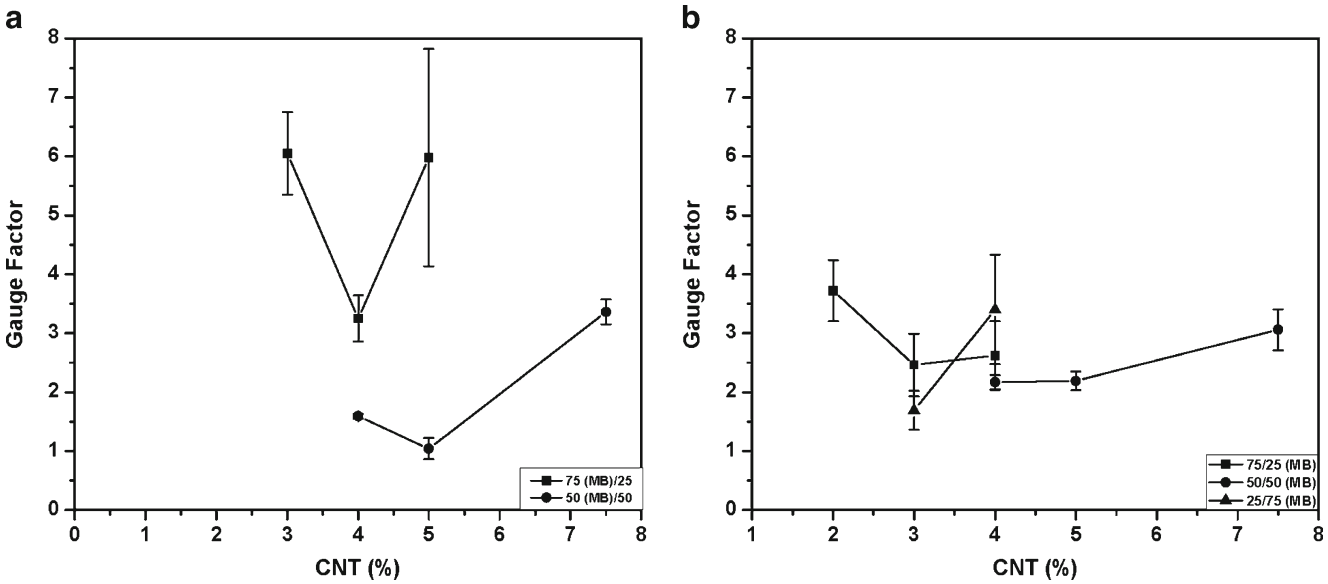

Fig. 6 Gauge Factor values for composites samples: a) 50(MB)/50 and 75(MB)/25 and b) 25/75(MB), 50/50(MB) and 75/25(MB) for several CNT contents

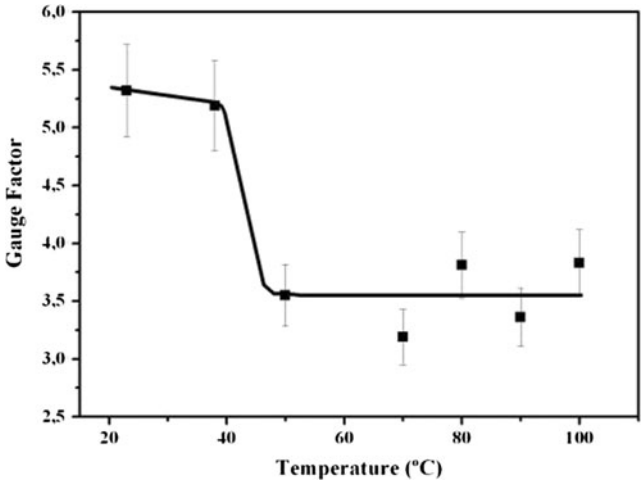

Fig. 7 Temperature dependence of Gauge Factor for composite 75(MB)/25/3. The line is for guiding the eyes

the filler network to a most favourable energy configuration and therefore less sensitive to mechanical variations.

The influence of the mechanical deformation speed on the GF is shown in Fig. 8. The GF is larger for low speeds (GF≈ 6), decreasing abruptly for deformations speeds above 5 mm/min. After these deformation the GF is practically independent of deformation speed up to deformations of 50 mm/min, the GF remaining in the rage $3.3 < GF < 4.7$. This behaviour is directly related to the time response of the semicrystalline polymer [27].

The maximum deformation of the composite sample also influences the piezoresistive response, the value of the GF increasing with increasing strain. For low strains the GF value is around zero and reaches values up to 6 at 1 mm displacement, indicative of the larger variations of resistance and therefore of sensor sensitivity for increasing mechanical deformations [27, 47].

Conclusions

In this work, the electrical, thermal and electromechanical behaviour of different CNT/polyamide composites were studied as function as their composition. The aim was to investigate the effect of matrix viscosity in the CNT dispersion and consequently, in the macroscopic properties of nanocomposites. The experimental data lead to the following conclusions:

- The PA66/PA6 ratio and the fact of the CNTs were originally pre-dispersed in a PA66 masterbatch or in a PA6 masterbatch are two factors which clearly influence the nanotube dispersion into the polyamide matrix.
- The morphologic study displays the best dispersion of MWCNTs was obtained when the polyamide ratio is rich in PA66 (the higher viscosity matrix) and the nanotubes are included from the lower viscosity masterbatch (PA6 MB).
- These nanocomposites with the best dispersion also achieved the best conductivity values.
- Respect to the thermal behaviour, the data show that in the case of composites with 75/25 and 25/75 polyamide ratios, the crystallization of the polyamide in lower proportion is inhibited by the presence of the fillers whereas if the polyamide ratio is 50/50, the crystallization of both polyamides is affected by the presence of the other one.
- The piezoresistive response of CNTs/PA composites depends on filler content and PA type concentration, being larger for composites with larger PA66 content.
- Regarding processing point of view, the inclusion of the CNT in the PA6 masterbatch helps to improve dispersion leading to larger values of the electrical conductivity when the polyamide ratio is rich in PA66.

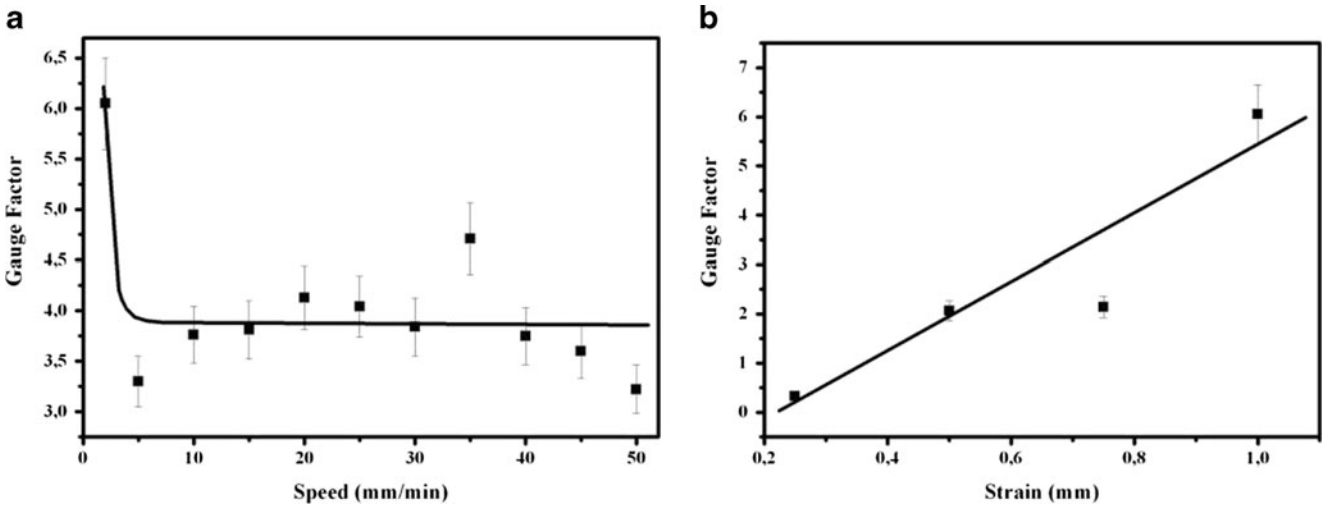

Fig. 8 **a** Mechanical deformation speed (fixed strain of 1 mm) and **b** strain (fixed speed of 1 mm/min) dependence of Gauge Factor for the 75(MB)/25/3 composite. The lines are for guiding the eyes

- On the other hand, Gauge Factors are better for the composites prepared from the PA66 masterbatch, besides the increase of PA66 content improving also the electromechanical response.
- Composite 75(MB)/25/3 reaches a GF value above 6 which indicates a main contribution from intrinsic piezoresistive effect and demonstrates the suitability of the materials for sensor applications.

Acknowledgements Authors acknowledge the financial support to MINECO-FEDER (research project IPT-420000-2010-004) and Xunta de Galicia-FEDER (Program of Consolidation and structuring competitive research units (CN2011/008).

L. Arboleda gratefully acknowledges financial support from Education Ministry with the program "Grants for students mobility stays for doctoral formation institutional strategies in Universities and consolidation of Doctorates programs with Excellence Mention".

Furthermore, this work was supported by FEDER through the COMPETE Program and by the Portuguese Foundation for Science and Technology (FCT) in the framework of the Strategic Project PEST-C/FIS/UI607/2011 and project PTDC/CTM-NAN/112574/2009. PC and AF also acknowledge FCT for the SFRH/BD/64267/2009 and SFRH/BD/69796/2010 grants, respectively. The authors also thank funding from Matepro –Optimizing Materials and Processes", ref. NORTE-07-0124-FEDER-000037", co-funded by the "Programa Operacional Regional do Norte" (ON.2 – O Novo Norte), under the "Quadro de Referência Estratégico Nacional" (QREN), through the "Fundo Europeu de Desenvolvimento Regional" (FEDER). Support from the COST Action MP1003, 2010 'European Scientific Network for Artificial Muscles' and MP0902 "Composites of Inorganic Nanotubes and Polymers, COINAPO" is also acknowledged.

References

1. Luo S, Liu T (2013) Structure–property–processing relationships of single-wall carbon nanotube thin film piezoresistive sensors. Carbon 59:315–324
2. György I (2008) Conductive polymers a new era in electrochemistry. Springer, Berlin Heidelberg
3. Hoppe H, Sariciftci NS (2004) Organic solar cells: an overview. J Mater Res 19(7):1924–1945
4. Zhang W, Dehghani-Sanij A, Blackburn RS (2007) Carbon based conductive polymer composites. J Mat Sci 42:3408–3418
5. Lorenz H, Fritzsche J, Das A et al (2009) Advanced elastomer nanocomposites based on CNT-hybrid filler systems. Compos Sci Technol 69:2135–2143
6. Du J-H (2007) The present status and key problems of carbon nanotube based polymer composites. Express Polym Lett 1:253–273
7. Ma P-C, Siddiqui NA, Marom G, Kim J-K (2010) Dispersion and functionalization of carbon nanotubes for polymer-based nanocomposites: a review. Compos A: Appl Sci Manuf 41:1345–1367
8. Sahoo NG, Rana S, Cho JW et al (2010) Polymer nanocomposites based on functionalized carbon nanotubes. Prog Polym Sci 35:837–867
9. Castillo FY, Socher R, Krause B et al (2011) Electrical, mechanical, and glass transition behavior of polycarbonate-based nanocomposites with different multi-walled carbon nanotubes. Polymer 52:3835–3845
10. Socher R, Krause B, Müller MT et al (2012) The influence of matrix viscosity on MWCNT dispersion and electrical properties in different thermoplastic nanocomposites. Polymer 53:495–504
11. Kelar K, Jurkowski B (2007) Properties of anionic polymerized ε-caprolactam in the presence of carbon nanotubes. J Appl Polym Sci 104:3010–3017
12. Saeed K, Park S (2007) Preparation of multiwalled carbon nanotube / nylon-6 nanocomposites by in situ polymerization. J Appl Polym Sci 106:3729–3735
13. Andrews R, Jacques D, Minot M, Rantell T (2002) Fabrication of carbon multiwall nanotube/polymer composites by Shear Mixing. Macromol Mater Eng 287:395
14. Hagerstrom JR, Greene SL (2000) Electrostatic dissipating composites containing Hyperion fibril nanotubes. Commercialization of nanostructured materials conference proceedings. Miami, Florida, USA, 6–7 April 2000
15. Ferguson DW, Bruant EWS, Fowler HC (1998) ESD thermoplastic product offers advantages for demanding electronic applications. ANTEC conference proceedings. Society of Plastics Engineers, Atlanta, pp 1219–1222
16. Pötschke P, Dudkin SM, Alig I (2003) Dielectric spectroscopy on melt processed polycarbonate—multiwalled carbon nanotube composites. Polymer 44:5023–5030
17. Mack C, Sathyanarayana S, Weiss P, et al. (2012) Twin-screw extrusion of multi walled carbon nanotubes reinforced polycarbonate composites: Investigation of electrical and mechanical properties. IOP Conf Ser: Model Simul Mater Sci Eng. doi:10.1088/1757-899X/40/1/012020
18. Pegel S, Pötschke P, Petzold G et al (2008) Dispersion, agglomeration, and network formation of multiwalled carbon nanotubes in polycarbonate melts. Polymer 49:974–984
19. Villmow T, Pegel S, Pötschke P, Wagenknecht U (2008) Influence of injection molding parameters on the electrical resistivity of polycarbonate filled with multi-walled carbon nanotubes. Compos Sci Technol 68:777–789
20. Paleo AJ, Sencadas V, Hattum FWJ Van (2013) Carbon nanofiber type and content dependence of the physical properties of carbon nanofiber reinforced polypropylene composites. Polymer Eng Sci 1–12. doi:10.1002/pen.23539
21. Cardoso P, Klosterman D, Covas JA et al (2012) Quantitative evaluation of the dispersion achievable using different preparation methods and DC electrical conductivity of vapor grown carbon nanofiber/epoxy composites. Polym Test 31:697–704
22. Xiao H, Li H, Ou J (2010) Sensors and actuators A: physical modeling of piezoresistivity of carbon black filled cement-based composites under multi-axial strain. Sensors Actuators: A Phys 160:87–93
23. Theodosiou TC, Saravanos DA (2010) Numerical investigation of mechanisms affecting the piezoresistive properties of CNT-doped polymers using multi-scale models. Compos Sci Technol 70:1312–1320
24. Oliva-Avilés AI, Avilés F, Sosa V (2011) Electrical and piezoresistive properties of multi-walled carbon nanotube/polymer composite films aligned by an electric field. Carbon 49:2989–2997
25. Chiacchiarelli LM, Rallini M, Monti M et al (2013) The role of irreversible and reversible phenomena in the piezoresistive behavior of graphene epoxy nanocomposites applied to structural health monitoring. Compos Sci Technol 80:73–79
26. Wang ZF, Wang P, Ye XY, Jiang B (2009) Processing and modeling of multi-walled carbon nanotube / styrene-butadiene-styrene (SBS) composites for force sensing. Nanotechnology, 2009 9th IEEE Conference on Nanotechnology 8:756–757
27. Ferreira A, Cardoso P, Klosterman D, Covas JA, Van Hattum FWJ, Vaz F, Lanceros-Mendez S (2012) Effect of filler dispersion on the electromechanical response of epoxy/vapor-grown carbon nanofiber composites. Smart Mater Struct. doi:10.1088/0964-1726/21/7/075008
28. Costa P, Silva J, Sencadas V et al (2012) Mechanical, electrical and electro-mechanical properties of thermoplastic elastomer styrene–

butadiene–styrene/multiwall carbon nanotubes composites. J Mat Sci 48:1172–1179
29. Slobodian P (2012) A highly-deformable composite composed of an entangled network of electrically-conductive carbon-nanotubes embedded in elastic polyurethane. Carbon 50:3446–3453
30. Krause B, Pötschke P, Häußler L (2009) Influence of small scale melt mixing conditions on electrical resistivity of carbon nanotube-polyamide composites. Compos Sci Technol 69:1505–1515
31. Timmaraju MV, Gnanamoorthy R, Kannan K (2011) Influence of imbibed moisture and organoclay on tensile and indentation behavior of polyamide 66/hectorite nanocomposites. Compos Part B: Eng 42: 466–472
32. Timmaraju MV, Gnanamoorthy R, Kannan K (2011) Effect of initial imbibed moisture content on flexural fatigue behavior of polyamide 66/hectorite nanocomposites at laboratory condition. Mater Sci Eng, A 528:2960–2966
33. Phang IY, Ma J, Shen L et al (2006) Crystallization and melting behavior of multi-walled carbon nanotube-reinforced nylon-6 composites. Polym Int 55:71–79
34. Logakis E, Pandis C, Peoglos V et al (2009) Structure—property relationships in polyamide 6 / multi-walled carbon nanotubes nanocomposites. J Polym Sci B Polym Phys 47:764–774
35. Bose S, Bhattacharyya AR, Kulkarni AR, Pötschke P (2009) Electrical, rheological and morphological studies in co-continuous blends of polyamide 6 and acrylonitrile–butadiene–styrene with multiwall carbon nanotubes prepared by melt blending. Compos Sci Technol 69:365–372
36. Bhattacharyya AR, Po P (2006) Mechanical properties and morphology of melt-mixed PA6 / SWNT composites: effect of reactive coupling. Macromol Symp 233:161–169
37. Edith Turi A (1997) Thermal characterization of polymeric materials, vol 2. Polytechnic University Brooklyn, New York
38. Menczel JD, Jaffe M, Bessey WE (1997) Thermal characterization of polymeric material. Academic, San Diego
39. Beeby S, Ensell G, Kraft M, White N (2004) MEMS mechanical sensors. Artech House, Boston
40. Zhu S, Chung DDL (2007) Analytical model of piezoresistivity for strain sensing in carbon fiber polymer–matrix structural composite under flexure. Carbon 45:1606–1613
41. Tomova D, Kressler J, Radusch H (2000) Phase behaviour in ternary polyamide 6 / polyamide 66 / elastomer blends. Polymer 41(21): 7773–7783
42. Li Y, Liu H, Zhang Y, Yang G (2005) Melting behavior and nonisothermal crystallization kinetics of polyamide 6/polyamide 66 molecular composites viain situ polymerization. J Appl Polym Sci 98:2172–2177
43. Caamaño C, Grady B, Resasco DE (2012) Influence of nanotube characteristics on electrical and thermal properties of MWCNT/ polyamide 6,6 composites prepared by melt mixing. Carbon 50: 3694–3707
44. Hu N, Karube Y, Yan C et al (2008) Tunneling effect in a polymer/ carbon nanotube nanocomposite strain sensor. Acta Mater 56:2929–2936
45. Del Castillo-castro T, Castillo-ortega MM, Herrera-franco PJ (2009) Composites: Part A Electrical, mechanical and piezo-resistive behavior of a polyaniline / poly (n-butyl methacrylate) composite. Compos Part A 40:1573–1579
46. Ferreira A, Rocha JG, Ansón-Casaos A et al (2012) Electromechanical performance of poly(vinylidene fluoride)/carbon nanotube composites for strain sensor applications. Sensors Actuators A Phys 178:10–16
47. Paleo AJ, Van Hattum FWJ, Rocha JG, Lanceros-Méndez S (2012) Piezoresistive polypropylene–carbon nanofiber composites as mechanical transducers. Microsyst Technol 18(5):591–597